Performance Evaluation of V2V Visible Light Communication: Coherence Time and Throughput in Motion Scenarios

Jinrui Hong, Xiayue Liu, Hanye Li, Yufei Jiang, *Member, IEEE*

Abstract—This study evaluates the performance of Vehicle-to-Vehicle Visible Light Communication in dynamic environments, focusing on the effects of speed, horizontal offset, and other factors on communication reliability. Using On-Off Keying modulation, we analyze the BER, optimal communication distance, correlation time and the maximum amount of data per communication. Our results demonstrate that maintaining an optimal vehicle distance is critical for stable communication, with speed and horizontal offset significantly influencing communication. This work extends the analysis of V-VLC to real-world dynamic scenarios, providing insights for future research.

Index Terms—Intelligent Transportation Systems, Vehicle-to-Vehicle, Correlation time, Visible Light Communication

I. INTRODUCTION

Intelligent transportation systems (ITS) improve road safety and traffic efficiency through real-time vehicle communication [1]. Current vehicle-to-vehicle (V2V) technologies include dedicated short-range communication (DSRC) and cellular vehicle-to-everything (C-V2X) [2]. However, these radio-frequency (RF) systems face challenges such as spectrum congestion [3]. Visible light communication in V2V scenarios (V-VLC), which uses vehicle LEDs as transmitters and photodiodes as receivers, offers a promising solution. V-VLC systems leverages the license-free visible light spectrum of 400–800 THz to avoid RF interference while reusing existing automotive lighting infrastructure [4]. By leveraging the unique advantages of V-VLC, this communication technology is being explored for various applications, including networked communication between automated guided vehicles (AGVs) in factory environments and between vehicles on the road.

Many studies investigate the system performance limits of V-VLC through channel modeling and analysis, which is crucial. While V-VLC channel modeling in indoor scenarios has been extensively studied [5], traffic scenarios present additional challenges, necessitating dedicated V-VLC channel models. Early works [6] used the line-of-sight (LOS) channel model, which is suitable for indoor LED luminaires but fails to capture the asymmetric intensity distributions of automotive headlamps. Headlamp intensity patterns were measured in [7] and used in VLC system performance analysis. [8] presented a closed-form path loss formula based on data fitting, but it is limited to clear weather conditions. Furthermore, [9] examined the impact of oscillations caused by vehicle motion in low-beam headlamp mode, demonstrating that these oscillations affect path loss.

(a) LED and PD pisition (b) Relative position of the vehicles
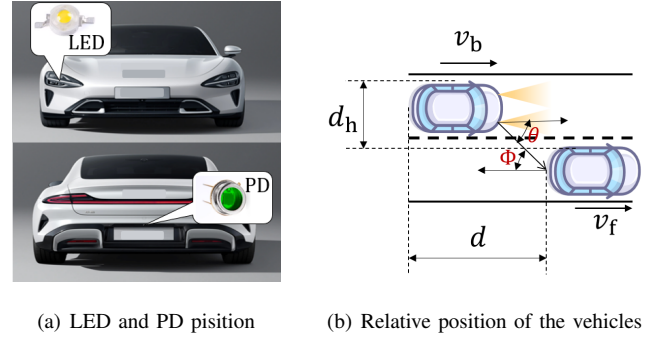
Fig. 1. System physical modeling: The geometric relationship between the device mounting location and the vehicle and the vehicle

However, in real-world V2V scenarios, vehicles are constantly in motion, a factor that has been largely overlooked in previous studies [5] [6] [7] [8]. Therefore, three key aspects of V-VLC during vehicle interactions are examined in this study: the successful completion of communication, the duration of communication, and the amount of data that can be transmitted. The main contributions of this paper are summarized as follows:

- We analyze a non-monotonic relationship between bit error rate (BER) and inter-vehicular positioning, where BER follows a U-shaped curve as a function of distance due to vehicle light radiation constraints. This reveals that optimal V-VLC communication occurs at specific intermediate distances rather than at minimum separation.
- We derive analytical expressions for correlation time and maximum achievable data throughput as functions of vehicular velocity, lateral displacement, and detection threshold parameters, establishing a theoretical framework for V-VLC performance prediction under dynamic conditions.

II. SYSTEM MODEL

Consider a single-input-single-output (SISO) V-V2X system. As shown in Fig. 1(a), the transmitter LED is mounted at the front center of the vehicles, while the receiver photodiode is placed at the rear center of the vehicles. The relative position of the vehicle can be modeled as Fig. 1(b).

In factory scenarios, without loss of generality, let d_h denotes the horizontal offset and d the inter-vehicle distance, as illustrated in Fig. 1(b). The channel model for factory V-V2V scenarios is expressed as [7]:

$$P_{\mathrm{L}} = 10\log\left(\frac{1}{2}\sum_{i=1}^{2}(\frac{\mathrm{k}}{L_i}\cos^m(\theta_i)\cos(\Phi_i)e^{(-cL_i)})\right) \quad (1)$$

where D_{R} denotes the receiver aperture diameter, m denotes the Lambertian radiation order which is related to the half-power angle, θ denotes the angle between the LED's normal direction and the observation direction, Φ denotes the angle between the PD plane and the observation direction, and c denotes the extinction coefficient, which quantifies the attenuation due to atmospheric factors per unit length. In this paper, $\log(x)$ denotes $\log_{10}(x)$ and $\exp(x)$ denotes e^x.

The channel model for V-V2V on the road scenarios is expressed as [7]:

$$P_{\mathrm{L}} = 10\log(\frac{1}{2}\sum_{i=1}^{2}(\frac{D_{\mathrm{R}}(\cos(\theta_i))^{\frac{1}{\epsilon}}}{\xi L_i})^2 \exp(-cL_i(\frac{D_{\mathrm{R}}}{\xi L_i})^{\frac{\epsilon}{2}})). \quad (2)$$

where ϵ and ξ denote the correction coefficients representing the asymmetric radiation pattern of vehicle lights and weather effects, and the definitions of other parameters, such as D_{R}, θ, Φ, and c, are consistent with the definitions in the factory scenario.

We consider two types of vehicle motion models. The car-following model of constant-speed assumes two vehicles separated by an initial distance d_0 moving at a constant relative velocity v, with one vehicle as the reference frame. The distance between two cars can be calculated as $d = d_0 + vt$.

The Pipe motion model [10] defines a scenario where the following vehicle's acceleration follows $a_{\mathrm{b}} = \frac{v_{\mathrm{f}} - v_{\mathrm{b}}}{T_{\mathrm{re}}}$, where v_{f} denotes the speed of the leading vehicle, v_{b} donates the following one, and T_{re} is a time parameter representing the driver's reaction time.

III. SYSTEM PERFORMANCE ANALYSIS

This section establishes a quantitative framework for evaluating vehicle optical communication systems through four key performance matrices: 1) Bit Error Rate (BER) quantifying signal integrity, let P_{e} denotes BER, 2) optimal communication distance S_{c} corresponding to the distance achieving minimal BER, 3) coherence time T_{c} defining the duration of reliable communication, and 4) maximum transmissible data volume L_{c}. Let $P_{\mathrm{e}}^{\mathrm{f}}$ denotes BER in factory scenatios and $P_{\mathrm{e}}^{\mathrm{r}}$ denotes BER in road scenatios. The meanings of $S_{\mathrm{c}}^{\mathrm{f}}$, $S_{\mathrm{c}}^{\mathrm{r}}$, $T_{\mathrm{c}}^{\mathrm{f}}$, $T_{\mathrm{c}}^{\mathrm{r}}$, $L_{\mathrm{c}}^{\mathrm{f}}$, $L_{\mathrm{c}}^{\mathrm{r}}$ are similar to BER situation.

A. Factory Scenarios

Proposition 1: Under the channel model for the factory scenario (1), using OOK modulation, the expressions for $P_{\mathrm{e}}^{\mathrm{f}}$ and $S_{\mathrm{c}}^{\mathrm{f}}$ can be derived as:

$$P_{\mathrm{e}}^{\mathrm{f}} = \frac{1}{2}\mathrm{erfc}(\frac{k\cos^m(\theta)\cos(\Phi)\exp(-cL)}{\sqrt{N}L}). \quad (3)$$

$$S_{\mathrm{c}}^{\mathrm{f}} = \frac{M^{\frac{1}{3}}}{6} - \frac{2(d_{\mathrm{h}})^2}{M^{\frac{1}{3}}}, \quad (4)$$

where $L = \sqrt{d^2 + d_{\mathrm{h}}^2}$ denotes the euclidean distance between LED and PD, $k = \frac{P_t D_{\mathrm{R}}^2(m+1)}{16\sqrt{2}}$ denotes the PD

aperture size and the radiation order of the light source, $M = 12\sqrt{12(d_{\mathrm{h}})^6 + 81(d_{\mathrm{h}})^4(m+2)^2} - 108(m+2)d_{\mathrm{h}}^2$. and $\mathrm{erfc(x)} = \frac{2}{\sqrt{\pi}}\int_0^x e^{-t^2}\,dt$.

Taking the derivative of the $P_{\mathrm{e}}^{\mathrm{f}}$ curve with respect to d and applying a mathematical identity transformation yields $S_{\mathrm{c}}^{\mathrm{f}3} + d_{\mathrm{h}}^2 S_{\mathrm{c}}^{\mathrm{f}} - d_{\mathrm{h}}^2(m+2) = 0$, it can be analyzed that as long as d_{h} is nonzero, the $P_{\mathrm{e}}^{\mathrm{f}}$ curve will always have an inflection point $S_{\mathrm{c}}^{\mathrm{f}}$. The reason for this phenomenon is: at short distances, angular misalignment causes high $P_{\mathrm{e}}^{\mathrm{f}}$, while at longer distances, the separation distance initially increasing $P_{\mathrm{e}}^{\mathrm{f}}$.

Proof: Based on the channel model for the factory scenario (1) and using OOK modulation, the $P_{\mathrm{e}}^{\mathrm{f}}$ is calculated via the formula: $P_{\mathrm{e}}^{\mathrm{f}} = \frac{1}{2}\mathrm{erfc}(\frac{A}{2\sqrt{2}\sigma})$ By substituting $A = \sqrt{P_{\mathrm{L}}P_t}$ and assuming a noise power of σ the $P_{\mathrm{e}}^{\mathrm{f}}$ expression is derived. ∎

Proposition 2: To define $T_{\mathrm{c}}^{\mathrm{f}}$ as the communication time range, we first determine the SNR threshold S_0. We define $T_{\mathrm{c}}^{\mathrm{f}} = |\{t|S_{(t)} > S_0\}|$, meaning that the time interval during which the SNR exceeds the threshold S_0 is considered the communication time range. Since the $P_{\mathrm{e}}^{\mathrm{f}}$ is directly related to the SNR under a given modulation scheme, this definition of $T_{\mathrm{c}}^{\mathrm{f}}$ is reasonable. Based on this mathematical definition, we calculate $T_{\mathrm{c}}^{\mathrm{f}}$ as:

$$T_{\mathrm{c}}^{\mathrm{f}} = \frac{\sqrt{\max\{0, T_0^f\}}}{v}. \quad (5)$$

where $T_0^f = \frac{D_{\mathrm{R}}^2 P_t(m+1)}{8 S_0 N} - 2(m+2)d_{\mathrm{h}}^2$.

Proof: Substituting P_{L} (2) into the defination of T_{c} yields:

$$\frac{P_t\frac{k}{L_i}\cos^m(\theta_i)\cos(\Phi_i)\exp(-cL_i)}{N} < S_0 \quad (6)$$

Assuming $\frac{d_{\mathrm{h}}^2}{(vt)^2}$ is negligible and applying a small-quantity approximation $(1+\alpha)^\beta = (1+\alpha\beta)$, $T_{\mathrm{c}}^{\mathrm{f}}$ is solved analytically. Considering the bandwidth limit B of vehicle headlamps with roll-off factor α, the maximum symbol rate is $R_{\max} = \frac{2B}{1+\alpha}$ to avoid ISI. Therefore, $L_{\mathrm{c}}^{\mathrm{f}} = R_{\max}T_{\mathrm{c}}^{\mathrm{f}}$. ∎

B. Road Scenarios

Proposition 3: Under the channel model for the road scenario (2), using OOK modulation, the expressions for $P_{\mathrm{e}}^{\mathrm{r}}$ and $S_{\mathrm{c}}^{\mathrm{r}}$ can be derived as:

$$P_{\mathrm{e}}^{\mathrm{r}} = \frac{1}{2}\mathrm{erfc}(\frac{Q\cos^{\frac{1}{\epsilon}}(\theta)\exp(-c\frac{L}{2})}{\sqrt{N}\xi L}). \quad (7)$$

$$S_{\mathrm{c}}^{\mathrm{r}} = \frac{F^{\frac{1}{3}}}{6} - \frac{2(d_{\mathrm{h}})^2}{F^{\frac{1}{3}}}, \quad (8)$$

where $Q = \frac{\sqrt{P_t}D_{\mathrm{R}}}{2\sqrt{2}}$ denotes the PD aperture size and the radiation order of the light source and the weather condition, $F = 12\sqrt{12(d_{\mathrm{h}})^6 + 81(d_{\mathrm{h}})^4(1+\frac{1}{\epsilon})^2} - 108(1+\frac{1}{\epsilon})d_{\mathrm{h}}^2$. Taking the derivative of the $P_{\mathrm{e}}^{\mathrm{r}}$ curve with respect to d yields $S_{\mathrm{c}}^{\mathrm{r}3} + d_{\mathrm{h}}^2 S_{\mathrm{c}}^{\mathrm{r}} - d_{\mathrm{h}}^2(\frac{1}{\epsilon}+1) = 0$ which is mathematically identical to the form in a factory scenario, it can be analyzed that the trend of the $P_{\mathrm{e}}^{\mathrm{r}}$ is consistent with the $P_{\mathrm{e}}^{\mathrm{f}}$ in factory scenarios.

(a) BER analysis   (b) T_c analysis
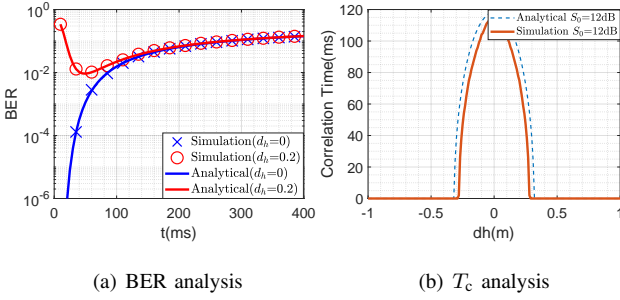
Fig. 2. Comparison of Theoretical and Simulated P_e^f and T_c^f in Factory Scenario

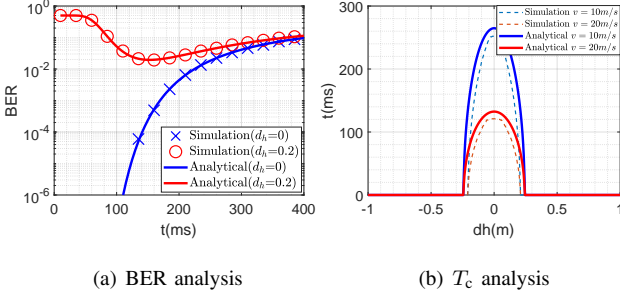(a) BER analysis   (b) T_c analysis

Fig. 3. Comparison of Theoretical and Simulated P_e^r and T_c^r in Factory Scenario

Proposition 4: In the road scenario, using a mathematical analysis method similar to that in the factory scenarios, we can derive the expression for T_c^r and L_c^r:

$$T_c^r = \frac{\sqrt{\max\{0, T_0^r\}}}{v}. \tag{9}$$

where $T_0^r = \frac{D_R^2 P_t}{\xi S_0 N} - \frac{2+2\epsilon}{\epsilon} d_h^2$.

IV. SIMULATION RESULTS

A. Simulation Setup

In this section, we conduct numerical simulations to verify the theoretical analysis.

In the factory scenarios(1), we set $D_R = 0.05$m, which means a 5cm diameter photodiode. For AGVs, $m = 5$ is adopted for the Lambertian radiation order, considering the small half-power angle due to headlamps primarily focusing on forward object detection. Under clear weather conditions, the extinction coefficient $c = 0.007$. And we set the horizontal offset d_h ranges from -1m to 1m.

In the road scenario(2), we keep parameters such as D_R, c and d_h consistent with the factory scenarios for later comparison, and we set $\epsilon = 0.15$ and $\xi = 0.17$.

B. Simulation Result And Discussion

As shown in Figs. 2(a) and Figs. 3(a), the P_e exhibits similar trends in both the factory and road scenarios: The P_e initially drops and then rises when d_h is nonzero, the optimal communication time occurs at the inflection point, which can be calculated using the formula in Section III. And the theoretical P_e matches the simulation results as is

shown in Fig. 2(a) and Fig. 3(a), confirming the accuracy of P_e theoretical formula.

The T_c variable also exhibits consistency in trends across different scenarios as is shown in Figs. 2(b) and Figs. 3(b): Fig. 2(b) shows that at $d_h = 0.2m$, T_c reduces to 70ms, and further decreases in d_h make communication impossible. Fig. 3(b) shows that the theoretical T_c formula matches the simulation results, confirming its accuracy too. It can also be seen from Fig. 3(b) that as v increases, T_c decreases, which is consistent with the analysis in Section III.

By comparing the T_c curves in the factory and road scenarios, it can be seen that under the same conditions, the T_c is longer and the P_e is lower in the road scenario. This is due to the headlamp's radiation pattern, which is more effective in directing light energy to farther distances.

V. CONCLUSION

This paper presents accurate formulas for BER, optimal communication distance, communication duration, and maximum data volume in V-VLC. We analyzes the impact of factors like horizontal offset and speed on communication performance. The study extends static V-VLC analysis to dynamic scenarios, providing valuable insights for future research. The findings emphasize the importance of maintaining an optimal distance between vehicles for stable communication and highlight the role of speed and horizontal offsets in data transmission efficiency.

REFERENCES

[1] M. Uysal, Z. Ghassemlooy, A. Bekkali, A. Kadri, and H. Menouar, "Visible light communication for vehicular networking: Performance study of a v2v system using a measured headlamp beam pattern model," *IEEE Vehicular Technology Magazine*, vol. 10, no. 4, pp. 45–53, Dec. 2015.

[2] F. Aghaei, H. B. Eldeeb, and M. Uysal, "A comparative evaluation of propagation characteristics of vehicular vlc and mmw channels," *IEEE Transactions on Vehicular Technology*, vol. 73, no. 1, pp. 4–13, Aug. 2024.

[3] P. Sharda and M. R. Bhatnagar, "Vehicular visible light communication system: Modeling and visualizing the critical outdoor propagation characteristics," *IEEE Transactions on Vehicular Technology*, vol. 72, no. 11, pp. 14 317–14 329, Jun. 2023.

[4] A. Memedi and F. Dressler, "Vehicular visible light communications: A survey," *IEEE Communications Surveys & Tutorials*, vol. 23, no. 1, pp. 161–181, Oct. 2021.

[5] F. Miramirkhani and M. Uysal, "Channel modeling and characterization for visible light communications," *IEEE Photonics Journal*, vol. 7, no. 6, pp. 1–16, Nov. 2015.

[6] M. Akanegawa, Y. Tanaka, and M. Nakagawa, "Basic study on traffic information system using led traffic lights," *IEEE Transactions on Intelligent Transportation Systems*, vol. 2, no. 4, pp. 197–203, Aug. 2001.

[7] M. Karbalayghareh *et al.*, "Channel modelling and performance limits of vehicular visible light communication systems," *IEEE Transactions on Vehicular Technology*, vol. 69, no. 7, pp. 6891–6901, May 2020.

[8] A. Memedi, H.-M. Tsai, and F. Dressler, "Impact of realistic light radiation pattern on vehicular visible light communication," in *GLOBECOM 2017 - 2017 IEEE Global Communications Conference*, Jan. 2017, pp. 1–6.

[9] B. Aly, M. Elamassie, and M. Uysal, "Vehicular visible light communication with low beam transmitters in the presence of vertical oscillation," *IEEE Transactions on Vehicular Technology*, vol. 72, no. 8, pp. 9692–9703, Mar. 2023.

[10] L. A. Pipes, "An operational analysis of traffic dynamics," *Journal of applied physics*, vol. 24, no. 3, pp. 274–281, Mar. 1953.